Wind Shear Estimation by Frequency-Shaped Optimal Estimator

B. K. Kim* and J. A. Bossi†
University of Washington, Seattle, Washington

This paper presents a formulation of the frequency-shaped optimal estimator and investigates the role of the measurement noise shaping function in this estimator. This shaping function creates transmission zeros and affects the singular values of the estimator transfer matrix, which can be used to improve control system robustness. The resulting estimator design technique has been applied to the estimation of wind shear onboard an airplane, and its performance has been simulated and compared with a reference Kalman filter.

Nomenclature

A	= system dynamics matrix
A_v, B_v, C_v, D_v	= realization matrices of measurement noise shaping function
A_w, B_w, C_w, D_w	= realization matrices of process noise shaping function
a_{hm}	= mean horizontal wind shear
$\hat{a}_{hm}$	= estimate of a_{hm}
B_c	= control distribution matrix
C	= measurement distribution matrix
c_t	= thrust coefficient
$F(s)$	= shaping filter transfer matrix
f_t	= wind turbulence characteristic frequency
G_c	= feedback control gain matrix
K, K_w, K_v	= gains of frequency-shaped estimator
Q	= spectral density matrix of process noise
$Q^{1/2}(s)$	= process noise shaping function
R	= spectral density matrix of measurement noise
$R^{1/2}(s)$	= measurement noise shaping function
r, r'	= estimator residuals
$\dot{r}_m$	= ground speed measurement
s	= Laplace transform frequency variable
$T_F(s)$	= estimator transfer matrix
t	= time
U_0	= equilibrium airspeed
u_a	= perturbed airspeed measurement
u_c	= control vector
V_{hm}	= mean horizontal wind speed
V_{ht}	= turbulence in horizontal wind
v, v'	= measurement noise vector, Gaussian white noise vector
w, w'	= process noise vector, Gaussian white noise vector
$\chi(\cdot)$	= stability derivatives for aircraft longitudinal axis
x, x_w, x_v, x_z	= state vectors of system and shaping filters
$\hat{x}, \hat{x}_w, \hat{x}_v, \hat{x}'$	= estimates of state vectors
y'	= output vector
$Z(\cdot)$	= stability derivatives for aircraft vertical axis
z	= measurement vector
δ_e	= elevator angle, deg
η_{ah}, η_{at}	= process noise components of wind dynamics
θ	= perturbed pitch angle
$\nu_{ua}, \nu_{\dot{r}}$	= measurement noise for airspeed and ground speed
$\Phi(s)$	= system dynamics transfer matrix
ω	= frequency

Received Dec. 27, 1983; revision received Sept. 13, 1985.

*Graduate Student, Department of Aeronautics and Astronautics. Student Member AIAA.

†Assistant Professor, Department of Aeronautics and Astronautics. Member AIAA.

Introduction

AUTOLAND control systems designed to maintain airspeed in the presence of wind shear tend to have large bandwidths that admit significant amounts of noise from wind turbulence through the airspeed measurement. This noise can produce unacceptable levels of control activity, particularly in thrust control. Previous research[1] has shown that onboard estimation of wind shear is possible by means of a steady-state Kalman filter; however, sufficiently responsive estimates still contain significant noise due to the first-order roll off characteristics of the Kalman filter.

Gupta[2] has proposed the use of frequency-shaped cost functionals in optimal estimator design to improve the frequency response characteristics of the estimate. These functionals result in additional dynamic states in the estimator, but these states need not be fed to the regulator in the complete control loop, so various estimator formulations could be used with the same regulator design.

Application of Gupta's approach to wind shear estimation requires careful selection of the frequency shaping functions since a robust estimator is necessary due to the inability to accurately define a dynamic model for all wind shear conditions. Safonov[3] and others have discussed the importance of the singular values of the system return difference matrix in determining system robustness. A reformulation of Gupta's noise-shaping transfer functions, described in this paper, shows that the poles of the measurement noise shaping function become transmission zeros of the estimator transfer matrix, which permits some control of the system singular values. Thus, robust estimation with good high-frequency attenuation can be achieved.

Subsequent sections describe the formulation of the frequency-shaped estimator, its application to wind shear modeling for a phugoid approximation of a typical transport airplane, and its simulated performance in a speed-hold system.

Frequency-Shaped Optimal Estimator

Consider the linear system:

$$\dot{x} = Ax + B_c u_c + w$$
$$z = Cx + v \tag{1}$$

As Gupta shows (Ref. 2 and references therein), the assumption of frequency-shaped cost functionals in the performance index can be implemented by treating w and v as autocorrelated noise sources generated by shaping filters of the form

$$w(j\omega) = Q^{1/2}(j\omega)w'(j\omega)$$
$$v(j\omega) = R^{1/2}(j\omega)v'(j\omega) \tag{2}$$

where Q and R are functions of the complex frequency $j\omega$ such that

$$Q(j\omega) = Q^{1/2}(j\omega)[Q^{1/2}(j\omega)]^*$$
$$R(j\omega) = R^{1/2}(j\omega)[R^{1/2}(j\omega)]^*$$

Here $Q^{1/2}$ and $R^{1/2}$ are rational functions of $j\omega$ (i.e. transfer matrices) and $[\,.\,]^*$ represents complex conjugation.

Gupta shows that for systems with states of finite amplitude, $Q^{1/2}$ must represent proper transfer functions (i.e., having at least as many poles as zeros), so that it can be realized by a dynamic system of the form

$$\dot{x}_w = A_w x_w + B_w w'$$
$$w = C_w x_w + D_w w' \tag{3}$$

However, $R^{1/2}(j\omega)$ is not similarly restricted; indeed, strictly proper transfer functions in $R^{1/2}$ would cause R to approach zero at high frequency, implying perfect measurements in that frequency range. Thus, for systems with realistic sensor models, the inverse filter $R^{-1/2}(j\omega)$ should be proper, and the measurement equations from Eq. (1) can be expressed, using Eq. (2), as

$$R^{-1/2}(j\omega)z(j\omega) = R^{-1/2}(j\omega)Cx(j\omega) + v'(j\omega) \tag{4}$$

Define a pseudomeasurement as

$$z'(j\omega) \equiv R^{-1/2}(j\omega)z(j\omega)$$

and a noise-free output as

$$y'(j\omega) \equiv R^{1/2}(j\omega)Cx(j\omega)$$

Then a dynamic realization of $R^{-1/2}$ can be formed as

$$\dot{x}_v = A_v x_v + B_v Cx$$
$$y' = C_v x_v + D_v Cx \tag{5}$$

with pseudomeasurement written as

$$z' = C_v x_v + D_v Cx + v' \tag{6}$$

Combining Eqs. (1), (3), (5), and (6) defines a dynamic system driven by independent white noise sources for which a constant-gain estimator (i.e., a steady-state Kalman filter) can be designed. This estimator can be represented by the equations

$$\dot{\hat{x}} = A\hat{x} + C_w\hat{x}_w + K[z' - C_v\hat{x}_v - D_vC\hat{x}] + B_c u_c$$
$$\dot{\hat{x}}_w = A_w\hat{x}_w + K_w[z' - C_v\hat{x}_v - D_vC\hat{x}]$$
$$\dot{\hat{x}}_v = A_v\hat{x}_v + B_vC\hat{x} + K_v[z' - C_v\hat{x}_v - D_vC\hat{x}] \tag{7}$$

where z' is obtained from z, using the realization of $R^{-1/2}(j\omega)$ in Eq. (5), by the equations

$$\dot{x}_z = A_v x_z + B_v z$$
$$z' = C_v x_z + D_v z \tag{8}$$

Thus, the designer's problem is to select $Q^{1/2}(j\omega)$ and $R^{-1/2}(j\omega)$, construct their realizations in Eqs. (3) and (5), and then design the estimator in Eq. (7) to meet performance requirements. The resulting estimator algorithm can be implemented by combining Eqs. (7) and (8). Letting $\hat{x}' = x_z - \hat{x}_v$, the implementation becomes

$$\dot{\hat{x}} = (A - KD_vC)\hat{x} + C_w\hat{x}_w + KC_v\hat{x}' + KD_vz + B_cu_c$$
$$\dot{\hat{x}}_w = A_w\hat{x}_w + K_wC_v\hat{x}' - K_wD_vC\hat{x} + K_wD_vz$$
$$\dot{\hat{x}}' = (A_v - K_vC_v)\hat{x}' - (B_v - K_vD_v)C\hat{x} + (B_v - K_vD_v)z \tag{9}$$

where measurements z are the input, and only $\hat{x}$ is fed to the regulator using, for example, the control law $u_c = G_c\hat{x}$. While techniques such as linear-quadratic synthesis can be used to obtain gains K, K_w, K_v, and G_c, the question of how to select the shaping filters remains. Since shaping filters add dynamic states to the estimator, the designer must trade performance and complexity in selecting the filters. Criteria for this selection can be developed based upon the effect of these filters on estimator frequency response; and, thus, on control loop robustness.

Transmission Zeros, Singular Values, and Robustness

For multivariable systems, frequency response characteristics are not as easily defined as for single-input/single-output (SISO) systems. However, theoretical efforts have been made to relate system robustness (i.e., margins of stability) to the magnitudes of the singular values[4] of return difference matrices.[3,5] These vary with frequency, and their values are influenced by the presence of transmission zeros in the loop. (Transmission zeros are the values of s at which an input signal produces no output.[6]) It can be shown, as is done in detail in Ref. 7, that measurement noise shaping can be used to insert transmission zeros in a multivariable loop at specified frequencies, altering the robustness of the loop.

This effect can be seen by taking the Laplace transform of Eq. (9) and formulating the block diagram of Fig. 1, where

$$r = z - C\hat{x} \quad \text{and} \quad r' = D_vr + C_v\hat{x}$$

Here, the transfer matrices for the system and each of the shaping filters, as obtained from Eqs. (1), (3), and (5), are represented by

$$\Phi(s) \equiv (sI - A)^{-1}$$

and, similarly, for $\Phi_w(s)$ and $\Phi_v(s)$. Note that the shaping filters form cascade elements for the standard estimator of Eq. (1), i.e. if $Q^{1/2}$ and $R^{1/2}$ are identity matrices and $K_w = K_v = 0$, then $r' = r$ and the steady-state Kalman filter results.

The feedback of K_v alters the poles of $\Phi_v(s)$, but the numerator polynomials of the transfer matrix from r to r' are preserved and thus appear in $T_F(s)$, the estimator transfer from z to $\hat{x}$. For the SISO case, this polynomial represents the zeros of $R^{-1/2}$ (i.e. the poles of $R^{1/2}$); and for the multivariable case, these polynomials can be shown to satisfy the definition of transmission zeros when $R^{-1/2}$ is diagonal.[7] To see this, Fig. 1 can be rearranged as shown in Fig. 2 where the measurement prefilter of Eq. (8) has been separated from the shaping filters in Eq. (7), which are represented by $F(s)$. Then, setting G_c to zero for convenience,

$$\hat{x}(s) = \Phi(s)F(s)R^{-1/2}(s)[z(s) - C\hat{x}(s)]$$

so that

$$T_F(s) = [I + \Phi(s)F(s)R^{-1/2}(s)C]^{-1}\Phi(s)F(s)R^{-1/2}(s)$$

Thus, $R^{-1/2}$ is a factor of T_F and, if it is diagonal with each element representing a SISO shaping function for a particular measurement, the zeros of $r_i^{-1/2}(s)$ will appear in the

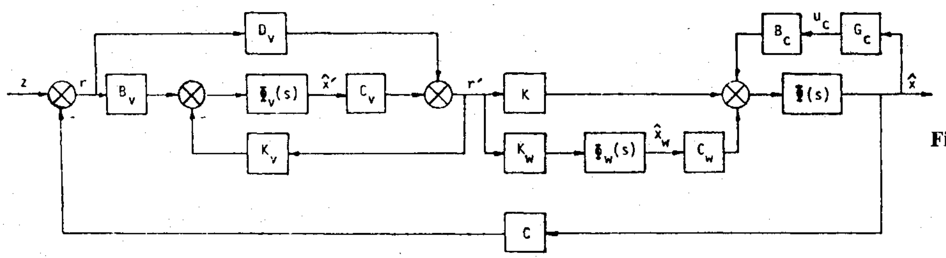

Fig. 1 Estimator block diagram for $T_F(s)$.

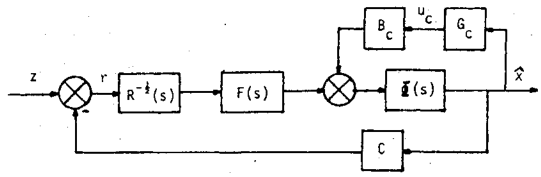

Fig. 2 Estimator diagram displaying cascaded pre-filter $R^{-1/2}(s)$.

numerators of all entries in the ith column of T_F. Therefore, classical SISO compensators can be used as measurement shaping filters and produce transmission zeros of the multivariable control loop at frequencies selected by the designer.

The capability to modify control loop singular values in specified ways by selection of these shaping functions is currently being investigated. However, the study reported in the next section showed that the introduction of lag compensation produces transmission zeros at high frequencies that reduce noise transmission while retaining good time response characteristics.

Wind Shear Estimation with Measurement Noise Shaping

The design and analysis procedure described above has been applied to a wind shear estimator for use in a typical speed-hold system for a large transport airplane in the landing approach condition. Only measurement noise shaping has been applied to introduce lag compensators for smoother estimates and system robustness. Performance of the resultant estimator has been analyzed and compared with a reference Kalman filter. Process noise shaping is being considered in further studies.

A phugoid approximation of airplane dynamics in the stability axis system has been selected for this analysis, i.e.,

$$\dot{u} = X_u u - q\theta/(57.3) - X_u V_{hm} - X_u V_{ht} + X_t c_t$$

$$\dot{\theta} = [57.3/(U_0 + Z_q)]\,(-Z_u u + Z_u V_{hm} + Z_u V_{ht} - Z_t c_t - Z_e \delta_e) \qquad (10)$$

The wind dynamics are taken from Refs. 1 and 8, with vertical wind velocity assumed to be zero and horizontal wind, approximated as parallel to the longitudinal axis, given by

$$\dot{V}_{hm} = a_{hm}$$

$$\dot{a}_{hm} = \eta_{ah}$$

$$\dot{V}_{ht} = -f_t V_{ht} + \sqrt{2 f_t}\,\eta_{at} \qquad (11)$$

where $f_t = 0.6\ \mathrm{s}^{-1}$ is used, which corresponds to a turbulence correlation length equivalent to the length of the airplane.

For the system model, $x = [u\theta V_{hm} a_{hm} V_{ht}]^T$ and $u_c = [\delta_e c_t]^T$ have been selected, and the airspeed and ground speed have been chosen as the measurements $z = [u_a \dot{r}_m]^T$ where

$$u_a = u - V_{hm} - V_{ht} + v_{ua}$$

$$\dot{r}_m = u + v_{\dot{r}} \qquad (12)$$

Table 1 Stability derivatives

$X_u = -0.04399$ 1/s	$Z_u = -0.2626$ 1/s
$X_t = 0.3321$ (ft/s^2)(1/unit)	$Z_t = -0.02142$ (ft/s^2)(1/unit)
$Z_q = 0$	$Z_e = -0.1382$ (ft/s)(1/deg)

Stability derivatives of a typical transport airplane at landing approach flight condition, as shown in Table 1, are used in this example with $U_0 = 240$ ft/s and a thrust of 5840 lb per unit of c_t.

For this sytem, a Kalman filter with a reasonable step response has been designed first, as a reference. Its performance is as shown in Fig. 3, which shows a rise time of 8-9 s and a significant level of noise at frequencies above 1 rad/s. If this estimator is used in closed-loop control of the airplane, however, the high frequency component of the power spectral density (PSD) will result in high frequency control activity.

To select measurement noise shaping functions, note that the transfer functions from horizontal wind to the measurements are, from the dynamics of Eq. (10),

$$z(s) = \begin{bmatrix} -\dfrac{s^2}{s^2 + 0.04s + 0.0342} \\ \dfrac{0.044(s + 0.78)}{s^2 + 0.04s + 0.0342} \end{bmatrix} (V_{hm} + V_{ht})$$

From this it is clear that in the frequency range of turbulence, the second measurement, ground speed, attenuates noise significantly; so major shaping needs to be applied to the first measurement, airspeed. It has been observed that rational functions of the same order in the numerator and denominator of the shaping function provide the most flexibility in estimator performance. Also, since higher order polynomials require more system states, the order should not be increased unnecessarily. Thus, polynomials of the second and the third orders from the classical Butterworth and ITAE filters[9] have been investigated, and the second order Butterworth pattern has been determined to be the most adequate for the numerator and the denominator of the shaping function.

As mentioned in the previous section, the introduction of lag compensation in $T_F(s)$ has been found to achieve smooth wind shear estimates. This requires a smaller corner frequency of the denominator than of the numerator in $r_i^{-1/2}(s)$, which implies that measurement noise $R(j\omega)$ should increase for frequencies above the denominator corner frequency. Therefore, this frequency needs to be greater than the operating frequency of the estimator to minimize the effects on the time response. Once the denominator is determined from these considerations, then the order of the polynomials and the corner

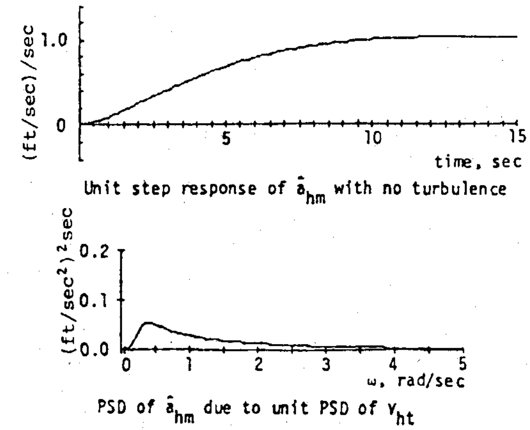

Fig. 3 Performance of the reference Kalman filter.

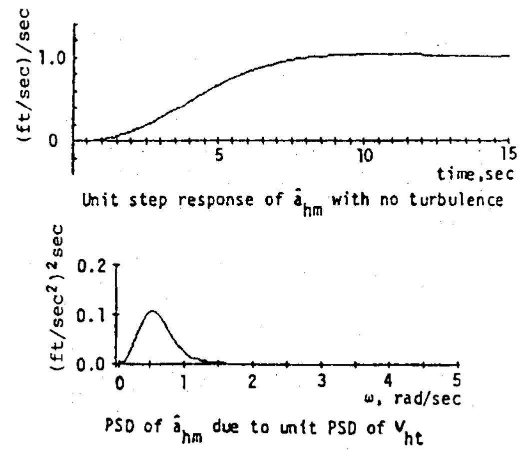

Fig. 4 Performance of the frequency-shaped estimator.

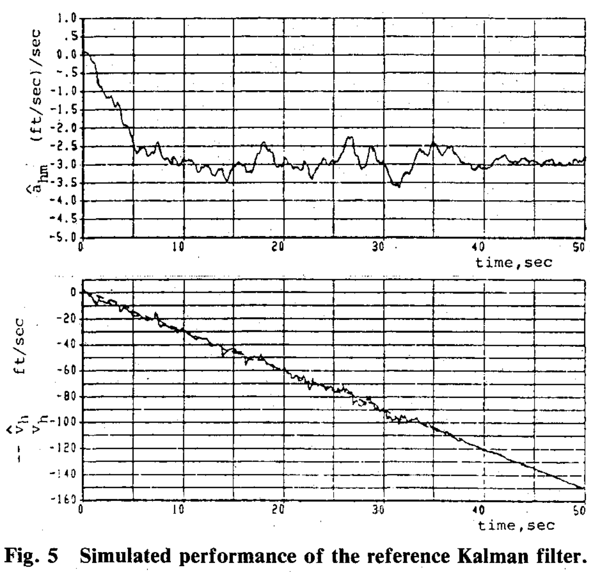

Fig. 5 Simulated performance of the reference Kalman filter.

Table 2 Estimator gain matrices

Ref. Kalman		Frequency-shaped K		Frequency-shaped K_V	
−0.048	0.266	−0.272	0.333	0.723	−0.082
0.058	−0.063	0.241	−0.084	0.812	−0.122
−1.119	0.313	−2.250	0.508	−0.045	0.163
−0.309	0.024	−0.573	0.063		
−0.665	0.0005	−0.241	0.013		

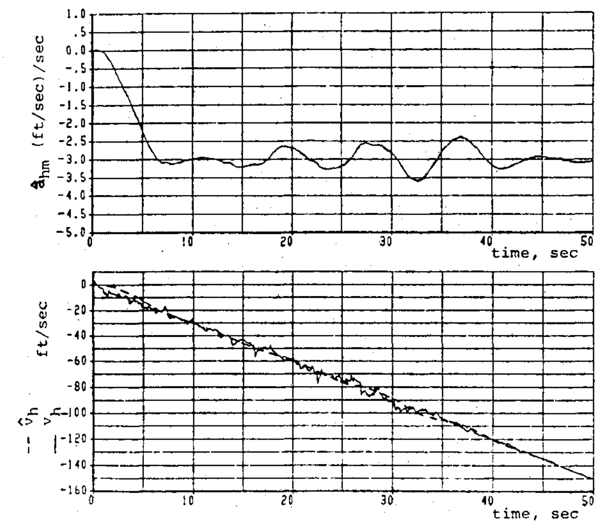

Fig. 6 Simulated performance of the frequency-shaped estimator.

Table 3 Control gain matrix G_c

−0.34	−3.96	0.34	0	0
−1.36	−4.06	1.36	3.0	0

frequency of the numerator determines the intensity of the noise assumed in the high frequency range.

Thus, since the phugoid frequency is roughly the operating range of the speed-hold system, the inverse of the shaping function for the first measurement noise has been selected to be

$$r_1^{-1/2}(s) = (s^2+2.8s+4.0)/16(s^2+0.7s+0.25)$$

which has corner frequencies at $\omega = 0.5$ and 2 rad/s and, therefore, assumes the noise to have a magnitude at higher frequency 16 times greater than at lower frequency.

Shaping the first measurement only with the above function has proved to provide good noise attenuation at high frequency. Further study[7] suggested that control loop robustness could be further improved by minor shaping applied to the second measurement, using a 1st-order function

$$r_2^{-1/2}(s) = (s+1.5)/3(s+0.5)$$

which assumes the noise to have three times greater magnitude at higher frequency than at lower frequency. The performance of the estimator using these noise shaping functions is shown in Fig. 4, which shows significant improvement in PSD of $\hat{a}_{hm}$ over the reference Kalman filter while maintaining the equivalent time response.

Figures 5 and 6 show the simulated performance of the reference Kalman filter and the frequency-shaped optimal estimator described above. Each estimator (see Table 2) has been inserted in a simulation of the autopilot system using the phugoid model of Eqs. (10-12) and a linear-quadratic regulator (see Table 3). For this simulation,

$$V_{hm} = -3t \text{ ft/s}$$

has been assumed, with the von Kármán turbulence of non-Gaussian distribution,[10,11] which represents a severe wind condition for landing approach.[1] As is clear from these simulation results, the frequency-shaped estimator exhibits a much smoother wind shear estimate while keeping the time response characteristics equivalent to those of the reference Kalman filter. A more extensive example for a full-order aircraft model is given in Ref. 7.

Conclusions

The results of this study indicate that frequency shaping of the measurement noise for an onboard estimation of wind shear can be effective in reducing the high frequency noise in the estimate while retaining good time response. These results are achieved by assigning transmission zeros of the estimator transfer function to an appropriate frequency band, which also influences control system robustness. The process of determining desired transmission zeros, based on desired noise attenuation, aids the selection of shaping functions to be used in the estimator. The relation of these functions to control loop robustness through the singular values of the return difference matrices is currently being studied.

Acknowledgment

This work has been supported by Boeing Commercial Airplane Company under contract Y-202431-0935N.

References

[1]Bossi, J. A. and Bryson, A. E., "Disturbance Estimation for a STOL Transport During Landing," *Journal of Guidance, Control, and Dynamics*, Vol. 5, May 1982, p. 258.

[2]Gupta, N. K., "Robust Control/Estimator Design by Frequency-shaped Cost Functionals," *Proceedings of IEEE Control and Decision Conference*, San Diego, CA, Dec. 1981, p. 1167.

[3]Safonov, M. G., Laub, A. J., and Hartmann, G. L., "Feedback Properties of Multivariable Systems: The Role and Use of the Return Difference Matrix," *IEEE Transactions on Automatic Control*, Vol. AC-26, Feb. 1981, p. 47.

[4]Strang, G., *Linear Algebra and its Applications*, 2nd ed., Academic Press, 1980, p. 286.

[5]Doyle, J. C. and Stein, G., "Multivariable Feedback Design: Concepts for a Classical/Modern Synthesis," *IEEE Transactions on Automatic Control*, Vol. AC-26, Feb. 1981, p. 4.

[6]Kailath, T., *Linear Systems*, Prentice-Hall, Inc., 1980, Sec. 6.5.

[7]Kim, B. K., "Frequency-shaped Estimation and Robust Controller Design for Aircraft Flight Control in Wind Disturbances," Ph.D. Dissertation, Department of Aeronautics and Astronautics, University of Washington, June 1983.

[8]Holley, W. E. and Bryson, A. E., "Wind Modeling and Lateral Control for Aircraft Landing," *Journal of Spacecraft and Rockets*, Vol. 14, Feb. 1977, pp. 65-72.

[9]Graham, D. and Lathrop, R. C., "Synthesis of Optimum Transient Response," *Transactions of AIEE*, Vol. 72, Part II, Nov. 1953, p. 273.

[10]Chan, Y. K., "Non-Gaussian von Karman Low Altitude Turbulence Simulation," Boeing Commercial Airplane Co. Document No. D6-48899 TN, April 1980.

[11]Chan, Y. K., "CN—An Update Program to Generate Correlated Random Numbers," Boeing Commercial Airplane Co. Document No. D6-48912 TN, April 1980.